

Temperature dependence of magnetization processes in $\text{Sm}(\text{Co},\text{Fe},\text{Cu},\text{Zr})_z$ magnets with different nanoscale microstructures - Supplements

Leonardo Pierobon^{1,*}, Robin E. Schäublin^{1,3}, András Kovács², Stephan S. A. Gerstl^{1,3}, Alexander Firlus¹, Urs V. Wyss⁴, Rafal E. Dunin-Borkowski², Michalis Charilaou^{1,5}, and Jörg F. Löffler^{1,*}

¹Laboratory of Metal Physics and Technology, Department of Materials, ETH Zurich, 8093 Zurich, Switzerland

²Ernst Ruska-Centre for Microscopy and Spectroscopy with Electrons, and Peter Grünberg Institute, Forschungszentrum Jülich, 52425 Jülich, Germany

³Scientific Center for Optical and Electron Microscopy, ETH Zurich, 8093 Zurich, Switzerland

⁴Arnold Magnetic Technologies, 5242 Birr-Lupfig, Switzerland

⁵Department of Physics, University of Louisiana at Lafayette, Lafayette, LA 70504, USA

*Leonardo Pierobon, leonardo.pierobon@mat.ethz.ch; Jörg F. Löffler, joerg.loeffler@mat.ethz.ch

Diffraction analysis of twinning in Sm–Co

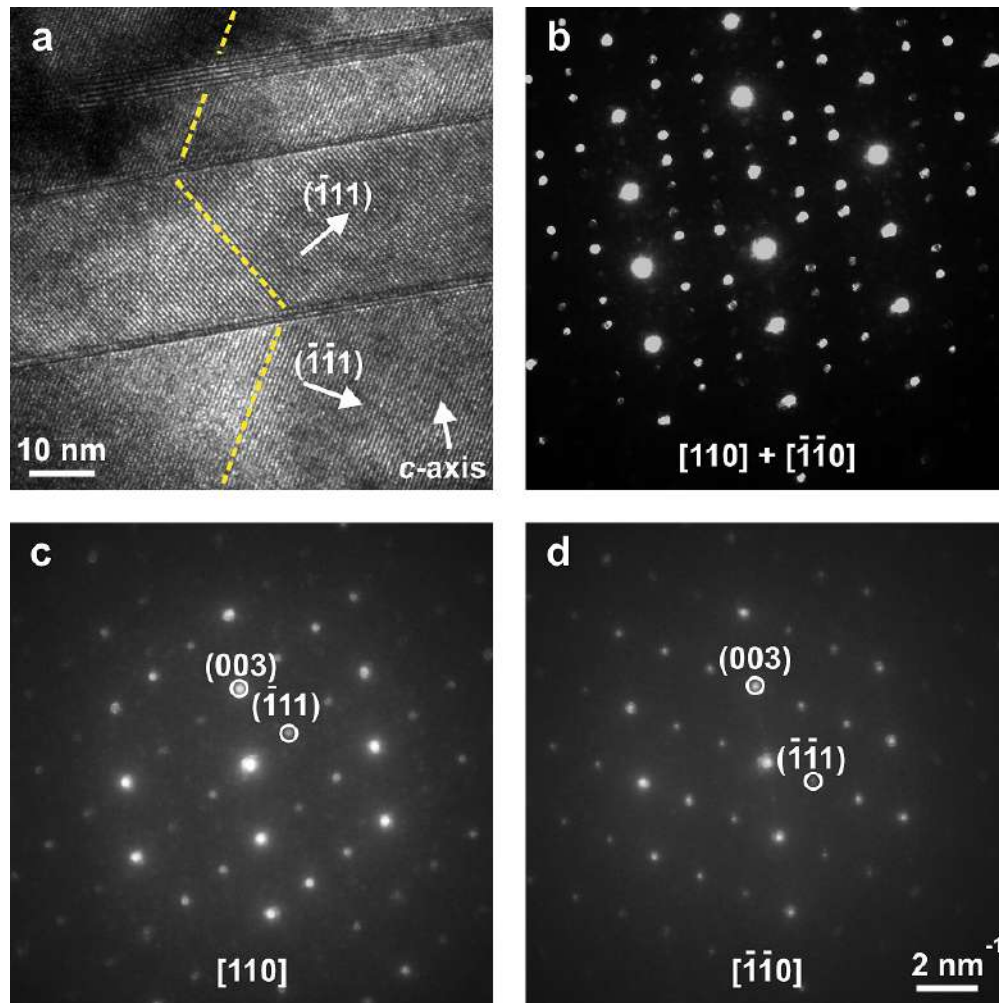
The crystal orientation of all the lamellae in the study was the same in order to ensure a consistent comparison between the samples. Supplementary Figure 1a shows a high-resolution transmission electron microscopy (TEM) image of $\text{Sm}^{\text{L}}\text{Cu}^{\text{L}}$, illustrating Z-phase platelets (diagonal lines) in $\text{Sm}_2\text{Co}_{17}$ cells. The thickness of the platelets varies significantly. The cells below and above the bottom and the middle platelets are in a twinning relationship, as indicated by the yellow dashed lines following the direction of the atomic planes. This is further confirmed by the diffraction patterns recorded across, above and below the bottom platelet shown in Supplementary Figures 1b, c and d, respectively. The patterns above and below contain the reflections from $[110]$ and $[\bar{1}\bar{1}0]$ directions, respectively, while the pattern across contains the reflections from both. The twinning of the cells at the Z phase is an abrupt discontinuity in the crystal structure and the magnetocrystalline anisotropy. This may significantly reduce the coercivity of the magnet.

APT analysis of the Z phase

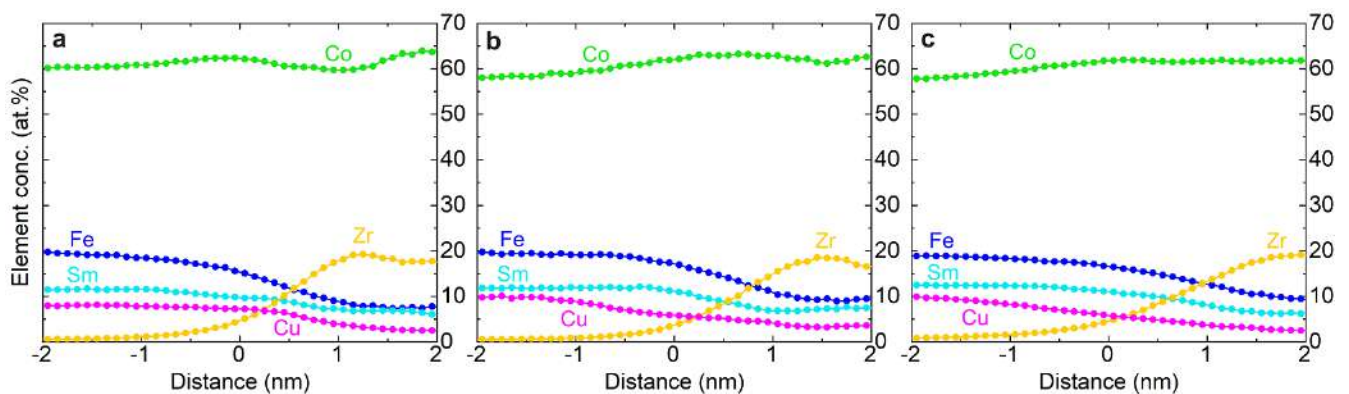
Atom probe tomography (APT) was used to obtain proxigrams (proximity histograms) of individual elements in the Z phase. Proxigrams show the concentration of elements as a function of distance from a predefined interface. In this case, the predefined interface corresponds to all surfaces with a Zr concentration of 5%, which are the edges of the Z phase. As shown in Supplementary Figure 2, the Zr distribution in all samples is almost identical, with the Zr concentration peaking at $19.3 \pm 0.2\%$ in $\text{Sm}^{\text{L}}\text{Cu}^{\text{L}}$, $18.7 \pm 0.4\%$ in $\text{Sm}^{\text{L}}\text{Cu}^{\text{H}}$ and $19.2 \pm 0.2\%$ in $\text{Sm}^{\text{H}}\text{Cu}^{\text{H}}$.

In-situ Lorentz TEM

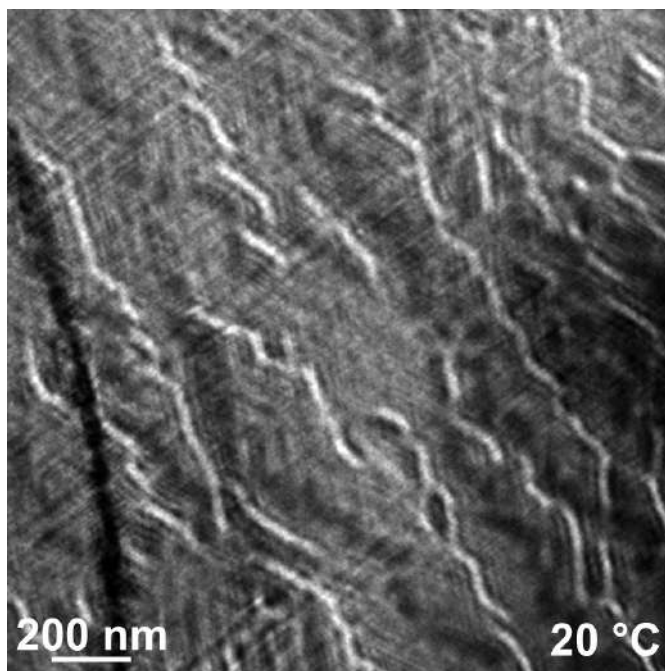
The magnetic structure of the samples was imaged in the Fresnel mode at $80 \mu\text{m}$ underfocus in an external magnetic field of 1.5 T applied by the objective lens perpendicular to the lamella (only perpendicular fields could be applied by the objective lens). Supplementary Video 1 shows for $\text{Sm}^{\text{L}}\text{Cu}^{\text{H}}$ the change in the magnetic texture from 20 to 400 °C. Specifically, the domain walls (DWs) indicated in Figures 5a,b in the main text are nucleated at 150 and 200 °C. The coercivity decreases with increasing the temperature, so the magnetization becomes saturated and DWs are annihilated by the external magnetic field above 200 °C, although some DWs survive up to 300 °C. When the sample is cooled back to 20 °C, it stays saturated perpendicular to the lamella (parallel to the external magnetic field).



Supplementary Figure 1. Twinning in Sm–Co. (a) High-resolution TEM image of the Z-phase platelets in $\text{Sm}_2\text{Co}_{17}$ cells, with yellow dashed lines indicating twinning across the platelets. Diffraction patterns recorded (b) across, (c) above and (d) below the bottom platelet contain the reflections from $[110]$ (panel c) and $[\bar{1}\bar{1}0]$ (panel d) directions, confirming the twinning.



Supplementary Figure 2. APT measurements of the Z phase. Proxigrams of individual elements with respect to the edges of the Z phase for (a) $\text{Sm}^{\text{L}}\text{Cu}^{\text{L}}$, (b) $\text{Sm}^{\text{L}}\text{Cu}^{\text{H}}$ and (c) $\text{Sm}^{\text{H}}\text{Cu}^{\text{H}}$, revealing that the element distribution across the Z phase is almost identical in all samples.



Supplementary Video 1. In-situ Lorentz TEM. Fresnel images of the magnetic structure of Sm^LCu^H at 80 μm underfocus in an external magnetic field of 1.5 T perpendicular to the lamella, showing DW nucleation at 150 and 200 °C and annihilation above 200 °C. The video is accessible online.